NRIAG Journal of Astronomy and Geophysics (2014) 3, 88–100

National Research Institute of Astronomy and Geophysics

NRIAG Journal of Astronomy and Geophysics

www.elsevier.com/locate/nrjag

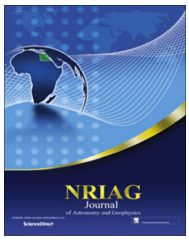

The astrophysical behavior of open clusters along the Milky Way Galaxy

A.L. Tadross *

National Research Institute of Astronomy & Geophysics, NRIAG, Elmarsad St., 11421 Helwan, Cairo, Egypt

Received 3 March 2014; revised 25 May 2014; accepted 1 June 2014
Available online 19 July 2014

KEYWORDS

Galaxy: open clusters and associations;
Astrometry;
Stars;
Astronomical databases: catalogs

Abstract The main aim of this paper is to study the astrophysical behaviour of open clusters' properties along the Milky Way Galaxy. Near-IR JHK_S (*2MASS*) photometry has been used for getting a homogeneous Catalog of 263 open clusters' parameters, which are randomly selected and studied by the author through the last five years; most of them were studied for the first time. The correlations between the astrophysical parameters of these clusters have been achieved by morphological way and compared with the most recent works.

1. Introduction

Open star clusters are very important objects in solving problems of star formation, stellar evolution, and improving our knowledge about the distance scale and the kinematic properties of the Milky Way Galaxy. This kind of study requires a large set of homogeneous data on the positions and ages of open star clusters, which are estimated in a precision way from their Colour-Magnitude Diagrams *(CMDs)*. However, it is useful to re-investigate the properties and structures of the Milky Way Galaxy using the most recent Near–IR JHK_S photometric data from the 2-Micron All Sky Survey (*2MASS*) Point Source Catalogue of Skrutskie (2006). In this context, we used a sample of 263 open star clusters (most of them are studied for the first time) that have been analysed by the author, in a series of papers; Tadross (2008–2012); see Tables 1 and 2. Our aim is to repeat the work we have done 12 years ago, Tadross (2001, 2002), to study such relations using NIR observations instead of UBV.

This paper is organized as follows. In Section 2, a historical review of the present study is obtained. In Section 3, data analysis of the clusters under investigation is presented. The limiting and core radii are given in Section 4. The main photometric parameters are obtained in Section 5. Ages and locations, distribution are presented in Section 6. Reddening distribution is presented in Section 7. The diameters and ages' relations are given in Sections 8 and 9, respectively. Sections 10 and 11 describe the spiral arms and warp of the Galaxy respectively. The conclusions are obtained in Section 12.

2. Historical review

Recently, Bukowiecki (2011) determined new coordinates of the centres, angular sizes and radial density profiles for 849

* Tel.: +20 2 25560645/25560046, mobile: +20 122 4095523; fax: +20 2 25548020.
E-mail address: altadross@yahoo.com.
Peer review under responsibility of National Research Institute of Astronomy and Geophysics.

2090-9977 © 2014 Production and hosting by Elsevier B.V. on behalf of National Research Institute of Astronomy and Geophysics.
http://dx.doi.org/10.1016/j.nrjag.2014.06.001

Table 1 The astrophysical main parameters for the studied clusters, derived by the author. Columns display, respectively, cluster name, equatorial positions, angular limiting radius, core radius, age, reddening, distance from the sun $R_{\odot}$, distance from the Galactic centre R_{gc}, the projected distances on the Galactic plane from the sun $X_{\odot}$, $Y_{\odot}$, Z, and the reference for each cluster.

Cluster		α			δ			$R_{lim.}$	R_c	Age	E_{B-V}	$R_{\odot}$	R_{gc}	$X_{\odot}$	$Y_{\odot}$	Z	Ref.
		h	*m*	*s*	°	′	″	′	′	*Gyr*	*mag*	*pc*	*kpc*	*pc*	*pc*	*pc*	
NGC	110	00	27	25	71	23	00	11.0	0.60	$0.9^{\pm 0.04}$	$0.46^{\pm 0.10}$	$1150^{\pm 53}$	9.14	585	975	172	6
NGC	272	00	51	24	35	49	54	3.2	0.29	$2.5^{\pm 0.10}$	$0.06^{\pm 0.02}$	$1068^{\pm 50}$	9.12	517	798	−486	6
NGC	657	01	43	21	55	50	11	3.0	0.90	$1.6^{\pm 0.11}$	$0.34^{\pm 0.05}$	$1372^{\pm 63}$	9.44	881	1041	−151	6
NGC	743	01	58	37	60	09	18	4.0	0.26	$0.5^{\pm 0.02}$	$0.95^{\pm 0.20}$	$1618^{\pm 75}$	9.64	1065	1217	−46	6
NGC	956	02	32	30	44	35	36	5.0	0.64	$1.0^{\pm 0.04}$	$0.10^{\pm 0.05}$	$1455^{\pm 67}$	9.68	1097	883	−367	6
NGC	1498	04	00	18	−12	00	54	3.8	0.68	$1.6^{\pm 0.11}$	$0.04^{\pm 0.02}$	$1020^{\pm 47}$	9.44	680	−297	−700	6
NGC	1520	03	57	51	−76	47	42	3.6	0.50	$2.0^{\pm 0.08}$	$0.06^{\pm 0.01}$	$775^{\pm 36}$	8.25	−227	−587	−452	6
NGC	1557	04	13	11	−70	28	18	13.0	0.10	$3.0^{\pm 0.12}$	$0.11^{\pm 0.05}$	$1055^{\pm 49}$	8.31	−197	−805	−653	6
NGC	1724	05	03	32	49	29	30	8.0	0.80	$0.6^{\pm 0.02}$	$0.57^{\pm 0.10}$	$1437^{\pm 66}$	9.85	1332	526	121	6
NGC	1785	04	58	35	−68	50	40	3.0	0.25	$0.5^{\pm 0.02}$	$0.06^{\pm 0.02}$	$3080^{\pm 140}$	8.52	−437	−2477	−1777	6
NGC	1807	05	10	43	16	31	18	9.0	0.46	$1.0^{\pm 0.04}$	$0.32^{\pm 0.05}$	$960^{\pm 44}$	9.46	928	−99	−224	6
NGC	1857	05	20	12	39	21	00	4.0	0.08	$0.16^{\pm 0.12}$	$0.97^{\pm 0.20}$	$1545^{\pm 71}$	10.02	1513	310	34	6
NGC	1891	05	21	25	−35	44	24	10.0	0.14	$2.0^{\pm 0.05}$	$0.03^{\pm 0.02}$	$860^{\pm 40}$	8.96	364	−624	−467	6
NGC	2013	05	44	01	55	47	36	3.0	0.32	$1.5^{\pm 0.06}$	$0.23^{\pm 0.05}$	$1100^{\pm 51}$	9.52	981	426	255	6
NGC	2017	05	39	17	−17	50	48	6.0	0.69	$1.6^{\pm 0.11}$	$0.06^{\pm 0.02}$	$1120^{\pm 52}$	9.37	767	−681	−450	6
NGC	2026	05	43	12	20	08	00	8.0	0.38	$0.55^{\pm 0.02}$	$0.60^{\pm 0.10}$	$1418^{\pm 65}$	9.91	1401	−178	−125	6
NGC	2039	05	44	00	08	41	30	5.0	0.36	$1.2^{\pm 0.05}$	$0.32^{\pm 0.05}$	$920^{\pm 42}$	9.38	863	−273	−164	6
NGC	2061	05	42	42	−34	00	34	9.0	0.96	$2.1^{\pm 0.08}$	$0.03^{\pm 0.01}$	$542^{\pm 25}$	8.79	246	−409	−256	6
NGC	2063	05	46	43	08	46	54	6.0	0.80	$1.3^{\pm 0.05}$	$0.32^{\pm 0.05}$	$1525^{\pm 70}$	9.97	1430	−445	−285	6
NGC	2132	05	55	18	−59	54	36	12.0	0.38	$1.65^{\pm 0.12}$	$0.06^{\pm 0.02}$	$974^{\pm 45}$	8.58	19	−842	−490	6
NGC	2165	06	11	04	51	40	36	5.0	0.44	$1.5^{\pm 0.06}$	$0.23^{\pm 0.05}$	$1445^{\pm 67}$	9.89	1328	427	377	6
NGC	2189	06	12	09	01	03	54	7.0	0.78	$0.8^{\pm 0.03}$	$0.39^{\pm 0.05}$	$1869^{\pm 86}$	10.19	1641	−853	−268	6
NGC	2219	06	23	44	−04	40	36	3.5	0.30	$0.8^{\pm 0.03}$	$0.40^{\pm 0.08}$	$2023^{\pm 93}$	10.24	1660	−1118	−292	6
NGC	2220	06	21	11	−44	45	30	6.5	0.40	$3.0^{\pm 0.12}$	$0.06^{\pm 0.01}$	$1170^{\pm 54}$	8.92	322	−1020	−475	6
NGC	2224	06	27	28	12	35	36	7.0	0.44	$0.01^{\pm 0.00}$	$1.00^{\pm 0.25}$	$2415^{\pm 111}$	10.81	2284	−785	23	6
NGC	2234	06	29	24	16	41	00	14.0	0.84	$0.8^{\pm 0.03}$	$0.51^{\pm 0.10}$	$1617^{\pm 75}$	10.07	1555	−434	79	6
NGC	2248	06	34	35	26	18	16	1.5	0.16	$1.0^{\pm 0.04}$	$0.23^{\pm 0.05}$	$1740^{\pm 80}$	10.23	1707	−226	250	6
NGC	2250	06	32	48	−05	02	00	2.0	0.29	$0.6^{\pm 0.02}$	$0.48^{\pm 0.10}$	$1795^{\pm 83}$	10.02	1456	−1031	−201	6
NGC	2260	06	38	03	−01	28	24	10.0	0.55	$0.01^{\pm 0.00}$	$1.25^{\pm 0.20}$	$1985^{\pm 90}$	10.23	1667	−1071	−126	6
NGC	2265	06	41	41	11	54	18	6.0	0.60	$0.3^{\pm 0.01}$	$0.48^{\pm 0.10}$	$2160^{\pm 100}$	10.54		−781	123	6
NGC	2312	06	58	47	10	17	42	3.8	0.18	$0.33^{\pm 0.01}$	$0.16^{\pm 0.05}$	$2245^{\pm 103}$	10.58	2030	−928	246	6
NGC	2318	06	59	27	−13	41	54	10.0	0.21	$0.05^{\pm 0.00}$	$0.65^{\pm 0.05}$	$1335^{\pm 62}$	9.48	924	−958	−104	6
NGC	2331	07	06	59	27	15	42	7.0	0.04	$1.7^{\pm 0.12}$	$0.06^{\pm 0.02}$	$1285^{\pm 59}$	9.77	1222	−210	337	6
NGC	2338	07	07	47	−05	43	12	3.5	0.21	$0.55^{\pm 0.02}$	$0.48^{\pm 0.05}$	$1800^{\pm 83}$	9.95	1381	−1154	32	6
NGC	2348	07	03	03	−67	24	42	5.0	0.33	$1.8^{\pm 0.07}$	$0.13^{\pm 0.05}$	$1070^{\pm 48}$	8.42	−139	−969	−432	6
NGC	2349	07	10	48	−08	35	36	9.0	0.55	$0.75^{\pm 0.03}$	$0.61^{\pm 0.10}$	$1628^{\pm 75}$	9.76	1195	−1106	10	6
NGC	2351	07	13	31	−10	29	12	5.0	0.49	$0.24^{\pm 0.01}$	$0.92^{\pm 0.25}$	$1882^{\pm 87}$	9.93	1336	−1325	2	6
NGC	2352	07	13	05	−24	02	18	3.0	0.90	$0.12^{\pm 0.00}$	$0.32^{\pm 0.15}$	$1750^{\pm 81}$	9.57	953	−1455	−191	6
NGC	2364	07	20	46	−07	33	00	6.5	0.50	$0.2^{\pm 0.01}$	$0.31^{\pm 0.05}$	$1919^{\pm 88}$	10.00	1401	−1307	101	6
NGC	2408	07	40	09	71	39	18	14.0	0.45	$3.0^{\pm 0.12}$	$0.03^{\pm 0.00}$	$1133^{\pm 52}$	9.44	794	585	557	6

(*continued on next page*)

Table 1 (*continued*)

Cluster		α			δ			$R_{lim.}$	R_c	Age	E_{B-V}	$R_\odot$	R_{gc}	$X_\odot$	$Y_\odot$	Z	Ref.
		h	*m*	*s*	°	′	″	′	′	*Gyr*	*mag*	*pc*	*kpc*	*pc*	*pc*	*pc*	
NGC	2455	07	49	01	−21	18	06	4.0	0.24	$0.18^{\pm 0.01}$	$0.54^{\pm 0.10}$	$2650^{\pm 122}$	10.14	1389	−2254	107	6
NGC	2459	07	52	02	09	33	24	2.7	0.04	$1.6^{\pm 0.11}$	$0.03^{\pm 0.02}$	$1300^{\pm 60}$	9.64	1060	−640	397	6
NGC	2587	08	23	25	−29	30	30	2.0	0.11	$0.1^{\pm 0.00}$	$0.23^{\pm 0.10}$	$1740^{\pm 80}$	9.26	609	−1624	136	6
NGC	2609	08	29	32	−61	06	36	2.5	0.06	$0.8^{\pm 0.03}$	$0.23^{\pm 0.10}$	$1320^{\pm 61}$	8.46	−138	−1280	−291	6
NGC	2666	08	49	47	44	42	12	5.5	0.30	$3.2^{\pm 0.13}$	$0.03^{\pm 0.01}$	$860^{\pm 40}$	9.36	664	47	544	6
NGC	2678	08	50	02	11	20	18	6.5	0.60	$2.3^{\pm 0.09}$	$0.03^{\pm 0.01}$	$900^{\pm 41}$	9.24	621	−452	469	6
NGC	2932	09	35	28	−46	48	36	10.5	0.07	$0.5^{\pm 0.02}$	$0.55^{\pm 0.10}$	$1525^{\pm 70}$	8.59	−47	−1521	103	6
NGC	2995	09	44	04	−54	46	48	3.5	0.70	$0.05^{\pm 0.00}$	$1.94^{\pm 0.30}$	$380^{\pm 17}$	8.46	−53	−376	−8	6
NGC	3231	10	26	58	66	48	55	3.5	0.47	$1.4^{\pm 0.06}$	$0.02^{\pm 0.00}$	$715^{\pm 33}$	9.07	401	314	502	6
NGC	3446	10	52	12	−45	08	54	7.5	0.97	$1.0^{\pm 0.04}$	$0.16^{\pm 0.05}$	$1485^{\pm 68}$	8.32	−298	−1417	329	6
NGC	3520	11	07	08	−18	01	24	1.5	0.24	$3.2^{\pm 0.13}$	$0.03^{\pm 0.00}$	$1245^{\pm 57}$	8.57	−13	−978	771	6
NGC	3909	11	49	49	−48	15	06	8.0	0.99	$2.0^{\pm 0.08}$	$0.13^{\pm 0.05}$	$1100^{\pm 50}$	8.14	−409	−989	254	6
NGC	4230	12	17	20	−55	06	06	5.0	0.07	$1.7^{\pm 0.12}$	$0.23^{\pm 0.10}$	$1445^{\pm 67}$	7.92	−673	−1265	187	6
NGC	5155	13	29	35	−63	25	30	8.5	0.08	$1.5^{\pm 0.18}$	$0.06^{\pm 0.02}$	$1070^{\pm 49}$	7.9	−647	−852	−16	6
NGC	5269	13	44	44	−62	54	54	1.5	0.02	$0.16^{\pm 0.11}$	$0.52^{\pm 0.10}$	$1410^{\pm 65}$	7.69	−886	−1096	−16	6
NGC	5299	13	50	26	−59	56	54	16.5	0.29	$2.0^{\pm 0.08}$	$0.19^{\pm 0.05}$	$1111^{\pm 50}$	7.83	−717	−847	40	6
NGC	5381	14	00	41	−59	35	12	5.5	0.67	$1.6^{\pm 0.11}$	$0.06^{\pm 0.02}$	$1170^{\pm 54}$	7.77	−776	−874	43	6
NGC	5800	15	01	47	−51	55	06	6.0	0.14	$0.9^{\pm 0.04}$	$0.62^{\pm 0.10}$	$2146^{\pm 99}$	6.92	−1692	−1301	222	6
NGC	5925	15	27	26	−54	31	42	12.0	0.12	$0.25^{\pm 0.01}$	$0.58^{\pm 0.10}$	$1040^{\pm 48}$	7.68	−845	−606	31	6
NGC	5998	15	49	34	−28	35	18	4.5	0.65	$2.2^{\pm 0.09}$	$0.16^{\pm 0.05}$	$981^{\pm 45}$	7.56	−886	−257	332	6
NGC	6334	17	20	49	−36	06	12	15.5	0.99	$0.5^{\pm 0.02}$	$1.06^{\pm 0.25}$	$1025^{\pm 47}$	7.49	−1013	−158	8	6
NGC	6357	17	24	43	−34	12	06	2.5	0.20	$0.4^{\pm 0.02}$	$1.35^{\pm 0.30}$	$1205^{\pm 55}$	7.3	−1196	−143	19	6
NGC	6360	17	24	27	−29	52	18	2.5	0.74	$0.02^{\pm 0.00}$	$1.11^{\pm 0.20}$	$1337^{\pm 62}$	7.17	−1333	−76	73	6
NGC	6374	17	32	18	−32	36	00	1.8	0.15	$1.3^{\pm 0.05}$	$0.48^{\pm 0.05}$	$900^{\pm 41}$	7.6	−897	−73	7	6
NGC	6421	17	45	44	−33	41	36	4.0	0.12	$0.17^{\pm 0.01}$	$1.26^{\pm 0.20}$	$1505^{\pm 69}$	7.0	−1500	−107	−63	6
NGC	6437	17	48	24	−35	21	00	7.5	0.31	$0.2^{\pm 0.01}$	$0.71^{\pm 0.05}$	$943^{\pm 43}$	7.56	−936	−91	−69	6
NGC	6507	17	59	50	−17	27	00	6.6	0.45	$0.40^{\pm 0.02}$	$0.85^{\pm 0.09}$	$1230^{\pm 55}$	7.3	−1203	246	65	1
NGC	6525	18	02	06	11	01	24	6.5	0.88	$2.0^{\pm 0.08}$	$0.14^{\pm 0.03}$	$1436^{\pm 66}$	7.46	−1097	838	393	6
NGC	6573	18	13	41	−22	07	06	0.9	0.15	$0.01^{\pm 0.00}$	$2.48^{\pm 0.20}$	$460^{\pm 21}$	8.05	−454	72	−17	6
NGC	6588	18	20	33	−63	48	30	2.5	0.13	$1.6^{\pm 0.11}$	$0.10^{\pm 0.03}$	$960^{\pm 44}$	7.68	−783	−437	−342	6
NGC	6595	18	17	04	−19	51	54	2.0	0.27	$0.45^{\pm 0.02}$	$0.94^{\pm 0.10}$	$1640^{\pm 76}$	6.90	−1607	325	−49	6
NGC	6605	18	18	21	−14	56	42	8.5	0.46	$0.6^{\pm 0.02}$	$0.52^{\pm 0.10}$	$889^{\pm 40}$	7.65	−855	244	5	6
NGC	6625	18	22	50	−11	57	42	7.7	0.22	$0.50^{\pm 0.03}$	$1.21^{\pm 0.13}$	$1335^{\pm 60}$	7.25	−1262	435	19	1
NGC	6645	18	32	37	−16	53	00	7.4	0.79	$0.40^{\pm 0.03}$	$0.36^{\pm 0.07}$	$1245^{\pm 55}$	7.31	−1195	338	−82	1
NGC	6647	18	32	50	−17	13	56	6.5	0.75	$1.60^{\pm 0.05}$	$0.54^{\pm 0.10}$	$2200^{\pm 100}$	6.4	−2119	577	−137	1
NGC	6659	18	33	59	23	35	42	7.0	0.11	$4.0^{\pm 0.16}$	$0.10^{\pm 0.03}$	$1155^{\pm 53}$	7.85	−682	888	282	6
NGC	6698	18	48	04	−25	52	42	5.5	0.40	$1.9^{\pm 0.07}$	$0.32^{\pm 0.05}$	$1150^{\pm 53}$	7.37	−1115	182	−215	6
NGC	6724	18	56	46	10	25	42	3.0	0.13	$0.9^{\pm 0.03}$	$1.00^{\pm 0.10}$	$1105^{\pm 51}$	7.73	−809	750	69	6
NGC	6735	19	00	37	00	28	30	6.0	0.03	$0.5^{\pm 0.02}$	$0.87^{\pm 0.15}$	$1466^{\pm 68}$	7.34	−1209	828	−47	6
NGC	6737	19	02	20	−18	32	59	4.4	0.41	$0.50^{\pm 0.02}$	$0.76^{\pm 0.11}$	$2120^{\pm 95}$	6.51	−1988	624	−392	1
NGC	6743	19	01	20	29	16	36	3.5	0.08	$1.4^{\pm 0.05}$	$0.19^{\pm 0.05}$	$1111^{\pm 51}$	8.01	−539	948	211	6
NGC	6773	19	15	03	04	52	54	4.3	0.12	$0.1^{\pm 0.00}$	$1.16^{\pm 0.20}$	$2160^{\pm 100}$	6.98	−1653	1386	−113	6
NGC	6775	19	16	48	−00	55	24	1.2	0.07	$0.9^{\pm 0.03}$	$0.48^{\pm 0.05}$	$1185^{\pm 55}$	7.58	−947	705	−108	6
NGC	6795	19	26	22	03	30	54	4.0	0.78	$0.95^{\pm 0.04}$	$0.45^{\pm 0.05}$	$1320^{\pm 61}$	7.54	−1004	845	−141	6

NGC	6815	19	40	44	26	45	30	15.0	0.10	$0.15^{\pm 0.01}$	$1.10^{\pm 0.20}$	$2024^{\pm 93}$	7.76	−945	1788	72	6
NGC	6832	19	48	15	59	25	18	12.0	0.11	$3.0^{\pm 0.12}$	$0.10^{\pm 0.02}$	$1750^{\pm 81}$	8.74	59	1678	493	6
NGC	6837	19	53	08	11	41	54	2.3	0.94	$1.0^{\pm 0.04}$	$0.25^{\pm 0.02}$	$943^{\pm 43}$	7.93	−594	721	−131	6
NGC	6839	19	54	33	17	56	18	3.0	0.90	$1.4^{\pm 0.05}$	$0.29^{\pm 0.05}$	$1410^{\pm 65}$	7.8	−−783	1166	−127	6
NGC	6840	19	55	18	12	07	36	3.0	0.04	$1.3^{\pm 0.04}$	$0.25^{\pm 0.05}$	$1970^{\pm 90}$	7.42	−1223	1518	−283	6
NGC	6843	19	56	06	12	09	48	2.5	0.26	$1.3^{\pm 0.04}$	$0.30^{\pm 0.05}$	$1945^{\pm 90}$	7.44	−1203	1501	−284	6
NGC	6846	19	56	28	32	20	54	2.4	0.12	$0.55^{\pm 0.02}$	$0.68^{\pm 0.05}$	$1445^{\pm 67}$	8.09	−525	1345	48	6
NGC	6847	19	56	37	30	12	48	10.0	0.74	$0.5^{\pm 0.02}$	$0.58^{\pm 0.05}$	$1894^{\pm 87}$	7.95	−743	1742	26	6
NGC	6856	19	59	17	56	07	48	1.6	0.08	$1.8^{\pm 0.06}$	$0.16^{\pm 0.02}$	$1704^{\pm 79}$	8.66	−9	1657	398	6
NGC	6858	20	02	56	11	15	30	5.0	0.59	$2.5^{\pm 0.10}$	$0.13^{\pm 0.02}$	$1310^{\pm 60}$	7.75	−805	1007	−234	6
NGC	6859	20	03	49	00	26	36	5.0	0.07	$3.0^{\pm 0.12}$	$0.19^{\pm 0.05}$	$1335^{\pm 62}$	7.56	−957	856	−364	6
NGC	6873	20	07	13	21	06	06	7.5	0.90	$0.88^{\pm 0.04}$	$0.35^{\pm 0.05}$	$1250^{\pm 58}$	7.96	−613	1081	−134	6
NGC	6895	20	16	29	50	13	48	8.0	0.85	$1.0^{\pm 0.04}$	$0.35^{\pm 0.05}$	$1141^{\pm 53}$	8.5	−81	1126	164	6
NGC	6904	20	21	48	25	44	24	4.0	0.69	$1.0^{\pm 0.04}$	$0.39^{\pm 0.05}$	$1355^{\pm 62}$	8.05	−545	1232	−149	6
NGC	6938	20	34	42	22	12	54	3.6	0.29	$1.3^{\pm 0.04}$	$0.13^{\pm 0.05}$	$1250^{\pm 58}$	8.05	−521	1112	−233	6
NGC	6950	20	41	04	16	37	06	7.5	0.41	$1.8^{\pm 0.05}$	$0.06^{\pm 0.02}$	$1070^{\pm 49}$	8.04	−499	904	−281	6
NGC	7005	21	01	57	−12	52	50	2.0	0.22	$2.5^{\pm 0.10}$	$0.03^{\pm 0.01}$	$1033^{\pm 48}$	7.69	−689	497	−588	6
NGC	7011	21	01	49	47	21	12	2.2	0.14	$0.4^{\pm 0.01}$	$1.08^{\pm 0.10}$	$1236^{\pm 57}$	8.55	−40	1235	13	6
NGC	7023	21	01	35	68	10	12	7.2	0.33	$0.12^{\pm 0.00}$	$1.10^{\pm 0.10}$	$560^{\pm 26}$	8.65	132	527	137	6
NGC	7024	21	06	09	41	29	18	2.5	0.23	$0.5^{\pm 0.02}$	$1.10^{\pm 0.10}$	$1760^{\pm 81}$	8.51	−175	1747	−119	6
NGC	7037	21	10	54	33	45	48	3.0	0.01	$2.1^{\pm 0.08}$	$0.16^{\pm 0.05}$	$1485^{\pm 68}$	8.35	−276	1437	−252	6
NGC	7050	21	15	12	36	10	24	3.5	0.45	$2.0^{\pm 0.08}$	$0.16^{\pm 0.05}$	$1179^{\pm 54}$	8.41	−171	1152	−180	6
NGC	7055	21	19	30	57	34	12	2.5	0.08	$0.8^{\pm 0.03}$	$1.10^{\pm 0.10}$	$1275^{\pm 59}$	8.76	165	1258	124	6
NGC	7071	21	26	39	47	55	12	4.0	0.15	$0.3^{\pm 0.01}$	$1.14^{\pm 0.20}$	$1684^{\pm 78}$	8.71	42	1682	−59	6
NGC	7084	21	32	33	17	30	30	8.0	0.90	$1.5^{\pm 0.06}$	$0.10^{\pm 0.05}$	$765^{\pm 35}$	8.27	−239	655	−315	6
NGC	7093	21	34	21	45	57	54	6.5	0.04	$0.9^{\pm 0.04}$	$0.61^{\pm 0.05}$	$1785^{\pm 82}$	8.72	32	1780	−135	6
NGC	7127	21	43	41	54	37	48	2.5	0.15	$0.4^{\pm 0.02}$	$0.90^{\pm 0.05}$	$1445^{\pm 67}$	8.82	199	1431	29	6
NGC	7129	21	42	59	66	06	48	3.5	0.21	$0.12^{\pm 0.01}$	$0.97^{\pm 0.05}$	$1070^{\pm 49}$	8.84	280	1016	184	6
NGC	7134	21	48	55	−12	58	24	1.5	0.10	$3.3^{\pm 0.13}$	$0.06^{\pm 0.02}$	$1065^{\pm 49}$	7.74	−558	502	−755	6
NGC	7175	21	58	46	54	49	06	16.0	0.18	$0.25^{\pm 0.01}$	$0.87^{\pm 0.05}$	$1930^{\pm 89}$	9.03	326	1902	−3	6
NGC	7193	22	03	03	10	48	06	6.5	0.39	$4.5^{\pm 0.18}$	$0.03^{\pm 0.00}$	$1080^{\pm 50}$	8.2	−304	839	−608	6
NGC	7352	22	39	43	57	23	42	4.5	0.03	$0.05^{\pm 0.00}$	$1.10^{\pm 0.20}$	$2550^{\pm 117}$	9.52	698	2452	−47	6
NGC	7394	22	50	23	52	08	06	4.5	0.20	$0.6^{\pm 0.02}$	$0.35^{\pm 0.05}$	$1310^{\pm 60}$	8.92	332	1259	−147	6
NGC	7429	22	56	00	59	58	24	7.0	0.06	$0.04^{\pm 0.00}$	$1.16^{\pm 0.10}$	$1190^{\pm 55}$	8.96	387	1125	6	6
NGC	7686	23	30	07	49	08	00	8.0	0.80	$2.0^{\pm 0.08}$	$0.20^{\pm 0.05}$	$1534^{\pm 71}$	9.13	502	1416	−307	6
NGC	7708	23	35	01	72	50	00	12.0	0.90	$2.0^{\pm 0.08}$	$0.42^{\pm 0.05}$	$1607^{\pm 74}$	9.35	726	1401	301	6
NGC	7795	23	58	37	60	02	06	10.5	0.19	$0.45^{\pm 0.02}$	$1.00^{\pm 0.10}$	$2105^{\pm 97}$	9.62	935	1885	−79	6
NGC	7801	00	00	21	50	44	30	4.0	0.98	$1.7^{\pm 0.12}$	$0.17^{\pm 0.05}$	$1275^{\pm 60}$	9.11	523	1136	−250	6
NGC	7826	00	05	17	−20	41	30	10.0	0.80	$2.2^{\pm 0.09}$	$0.03^{\pm 0.01}$	$620^{\pm 29}$	8.23	−62	117	−606	6
NGC	7833	00	06	31	27	38	30	1.3	0.10	$2.0^{\pm 0.08}$	$0.06^{\pm 0.02}$	$1410^{\pm 65}$	9.10	416	1090	−792	6
Berkeley	1	00	09	36	60	28	30	2.5	0.14	$0.4^{\pm 0.03}$	$0.78^{\pm 0.06}$	$2420^{\pm 110}$	9.9	1128	2139	−84	2
Berkeley	6	01	51	11	61	03	40	3.0	0.15	$0.1^{\pm 0.00}$	$0.78^{\pm 0.05}$	$2300^{\pm 105}$	10.1	1481	1759	−38	2
Berkeley	26	06	50	18	05	45	00	2.6	0.13	$0.6^{\pm 0.03}$	$0.54^{\pm 0.05}$	$2720^{\pm 120}$	11.0	2407	−1262	112	2
Berkeley	37	07	20	24	−01	06	00	3.5	0.69	$0.9^{\pm 0.04}$	$0.12^{\pm 0.02}$	$4555^{\pm 210}$	12.4	3605	−2740	470	2
Berkeley	43	19	15	36	11	13	00	4.5	0.57	$0.4^{\pm 0.03}$	$1.52^{\pm 0.14}$	$1355^{\pm 60}$	7.6	−947	969	−4	2
Berkeley	45	19	19	12	15	43	00	3.5	0.14	$0.6^{\pm 0.03}$	$0.82^{\pm 0.05}$	$2300^{\pm 105}$	7.2	−1477	1763	46	2

(*continued on next page*)

Table 1 (*continued*)

Cluster		α			δ			$R_{lim.}$	R_c	Age	E_{B-V}	$R_\odot$	R_{gc}	$X_\odot$	$Y_\odot$	Z	Ref.
		h	*m*	*s*	°	′	″	′	′	*Gyr*	*mag*	*pc*	*kpc*	*pc*	*pc*	*pc*	
Berkeley	47	19	28	36	17	22	06	2.0	0.03	$0.16^{\pm 0.01}$	$1.06^{\pm 0.10}$	$1420^{\pm 65}$	7.7	−863	1127	−1.4	2
Berkeley	49	19	59	31	34	38	48	2.4	0.17	$0.16^{\pm 0.01}$	$1.57^{\pm 0.30}$	$2035^{\pm 110}$	8.1	−662	1922	91	2
Berkeley	50	20	10	24	34	58	00	3.5	0.12	$0.25^{\pm 0.01}$	$0.97^{\pm 0.07}$	$2100^{\pm 100}$	8.1	−633	2002	31	2
Berkeley	51	20	11	54	34	24	06	1.5	0.13	$0.15^{\pm 0.02}$	$1.66^{\pm 0.14}$	$3200^{\pm 145}$	8.1	−981	3046	16	2
Berkeley	61	00	48	30	67	12	00	3.5	0.19	$0.8^{\pm 0.05}$	$1.09^{\pm 0.11}$	$3335^{\pm 150}$	10.7	1794	2800	252	2
Berkeley	63	02	19	36	63	43	00	3.6	0.35	$0.5^{\pm 0.02}$	$0.90^{\pm 0.09}$	$3305^{\pm 150}$	11.0	2231	2434	144	2
Berkeley	72	05	50	18	22	12	00	3.5	0.08	$0.6^{\pm 0.02}$	$0.79^{\pm 0.07}$	$3810^{\pm 175}$	12.3	3783	−419	−171	2
Berkeley	76	07	06	40	−11	44	00	4.5	0.96	$0.8^{\pm 0.04}$	$0.73^{\pm 0.05}$	$2505^{\pm 115}$	10.4	1764	−1770	−87	2
Berkeley	84	20	04	43	33	54	18	1.1	0.06	$0.12^{\pm 0.01}$	$0.76^{\pm 0.05}$	$2025^{\pm 95}$	8.1	−661	1912	45	2
Berkeley	89	20	24	36	46	03	00	2.5	0.08	$0.85^{\pm 0.05}$	$1.03^{\pm 0.10}$	$3005^{\pm 135}$	8.7	−357	2973	253	2
Berkeley	90	20	35	18	46	50	00	2.5	0.22	$0.1^{\pm 0.01}$	$1.15^{\pm 0.10}$	$2430^{\pm 70}$	8.6	−216	2415	160	2
Berkeley	91	21	10	52	48	32	12	1.7	0.13	$0.5^{\pm 0.02}$	$1.00^{\pm 0.09}$	$2400^{\pm 110}$	8.8	2.7	2400	5.5	2
Berkeley	95	22	28	18	59	08	00	2.4	0.29	$0.15^{\pm 0.02}$	$1.21^{\pm 0.12}$	$1900^{\pm 85}$	9.2	507	1830	40	2
Berkeley	97	22	39	30	59	01	00	2.0	0.10	$0.02^{\pm 0.00}$	$0.75^{\pm 0.05}$	$1800^{\pm 85}$	9.2	516	1724	12	2
Berkeley	100	23	25	58	63	46	48	2.2	0.29	$0.16^{\pm 0.01}$	$1.21^{\pm 0.11}$	$3355^{\pm 155}$	10.3	1345	3070	144	2
Berkeley	101	23	32	47	64	12	30	2.2	0.23	$0.7^{\pm 0.05}$	$1.11^{\pm 0.10}$	$2500^{\pm 115}$	9.8	1036	2272	115	2
Berkeley	102	23	38	42	56	38	00	3.3	0.28	$0.6^{\pm 0.03}$	$0.69^{\pm 0.05}$	$2600^{\pm 120}$	9.8	1013	2384	−219	2
Berkeley	103	23	45	12	59	18	00	2.5	0.36	$0.5^{\pm 0.02}$	$1.00^{\pm 0.11}$	$2100^{\pm 95}$	9.6	872	1908	−91	2
Kronberger	2	18	21	19	−14	17	12	2.5	0.08	$0.10^{\pm 0.00}$	$1.10^{\pm 0.10}$	$3065^{\pm 140}$	5.6	−2934	887	1.5	4
Kronberger	3	19	39	00	06	46	00	1.0	0.03	$1.60^{\pm 0.11}$	$0.38^{\pm 0.08}$	$1870^{\pm 85}$	7.3	−1324	1299	−240	4
Kronberger	5	19	46	05	27	50	00	3.5	0.08	$0.16^{\pm 0.02}$	$2.10^{\pm 0.40}$	$615^{\pm 30}$	8.2	−273	551	17	4
Kronberger	12	06	14	16	22	29	52	1.4	0.17	$0.16^{\pm 0.02}$	$0.97^{\pm 0.05}$	$1775^{\pm 80}$	10.3	1753	−271	74	4
Kronberger	13	19	25	15	13	56	44	1.2	0.08	$0.40^{\pm 0.01}$	$1.13^{\pm 0.11}$	$1380^{\pm 65}$	7.7	−902	1044	−24	4
Kronberger	18	05	18	36	37	37	18	4.0	0.36	$0.10^{\pm 0.00}$	$1.29^{\pm 0.12}$	$3250^{\pm 150}$	11.7	3197	584	1.9	4
Kronberger	23	23	05	59	60	15	14	0.9	0.15	$0.10^{\pm 0.01}$	$1.35^{\pm 0.12}$	$1740^{\pm 80}$	9.2	601	1633	0.44	4
Kronberger	25	18	22	40	−14	43	41	0.8	0.10	$0.05^{\pm 0.00}$	$1.32^{\pm 0.11}$	$1220^{\pm 55}$	7.3	−1169	348	−10	4
Kronberger	28	20	06	32	35	34	34	0.75	0.09	$0.40^{\pm 0.01}$	$2.26^{\pm 0.42}$	$550^{\pm 25}$	8.4	−165	524	18	4
Kronberger	52	19	58	08	30	53	18	1.2	0.06	$0.13^{\pm 0.01}$	$2.45^{\pm 0.44}$	$705^{\pm 30}$	8.3	−268	652	10.5	4
Kronberger	54	20	03	08	31	58	01	0.8	0.11	$0.25^{\pm 0.02}$	$0.94^{\pm 0.04}$	$1715^{\pm 80}$	8.0	−612	1602	15.5	4
Kronberger	55	23	53	09	62	47	12	1.1	0.07	$0.40^{\pm 0.02}$	$1.13^{\pm 0.11}$	$1260^{\pm 60}$	9.1	559	1129	15	4
Kronberger	57	20	23	58	36	36	17	2.2	0.16	$0.16^{\pm 0.02}$	$1.06^{\pm 0.09}$	$1295^{\pm 60}$	8.3	−328	1253	−11	4
Kronberger	58	20	20	48	41	12	17	0.25	0.01	$0.16^{\pm 0.02}$	$1.35^{\pm 0.12}$	$1515^{\pm 70}$	8.3	−295	1484	69.5	4
Kronberger	59	20	23	50	40	08	53	1.0	0.04	$0.10^{\pm 0.00}$	$0.84^{\pm 0.11}$	$780^{\pm 35}$	8.4	−144	766	0.05	4
Kronberger	60	06	04	10	31	29	44	1.6	0.12	$0.80^{\pm 0.03}$	$0.84^{\pm 0.11}$	$1960^{\pm 90}$	10.5	1953	6.6	162	4
Kronberger	68	20	00	36	30	35	23	2.2	0.18	$0.20^{\pm 0.03}$	$2.19^{\pm 0.40}$	$710^{\pm 30}$	8.2	−270	567	3.1	4
Kronberger	72	20	12	19	37	53	27	2.0	0.23	$0.50^{\pm 0.02}$	$0.55^{\pm 0.08}$	$1055^{\pm 50}$	8.3	−271	1019	39	4
Kronberger	73	20	13	47	36	44	55	1.2	0.09	$0.40^{\pm 0.02}$	$0.97^{\pm 0.05}$	$1695^{\pm 80}$	8.2	−458	1632	37	4
Kronberger	74	20	17	57	36	45	37	1.1	0.05	$1.00^{\pm 0.04}$	$0.87^{\pm 0.05}$	$1760^{\pm 80}$	8.2	−462	1698	18	4
Kronberger	80	21	11	50	52	22	48	1.7	0.16	$0.70^{\pm 0.03}$	$1.29^{\pm 0.10}$	$1355^{\pm 60}$	8.7	69	1352	66	4
Kronberger	84	21	35	32	53	30	49	2.2	0.19	$0.60^{\pm 0.02}$	$0.61^{\pm 0.07}$	$1075^{\pm 50}$	8.7	117	1068	21	4
Kronberger	85	07	58	21	−34	46	11	1.5	0.11	$0.30^{\pm 0.01}$	$1.00^{\pm 0.10}$	$1525^{\pm 70}$	9.1	497	−1440	−76	4
Czernik	1	00	07	38	61	28	30	2.5	0.12	$0.005^{\pm 0.00}$	$1.23^{\pm 0.11}$	$2530^{\pm 115}$	9.9	1177	2239	−42	4
Czernik	2	00	43	42	60	09	00	5.8	0.08	$0.10^{\pm 0.01}$	$0.74^{\pm 0.12}$	$1775^{\pm 80}$	9.6	939	1504	−84	4
Czernik	3	01	03	06	62	47	00	2.4	0.14	$0.10^{\pm 0.01}$	$1.42^{\pm 0.14}$	$1410^{\pm 65}$	9.4	794	1165	−1.4	4

Czernik	4	01	35	24	61	26	00	2.6	0.77	$0.10^{\pm 0.01}$	$1.06^{\pm 0.10}$	$1630^{\pm 75}$	9.6	1007	1281	−28	4
Czernik	5	01	55	06	61	20	00	1.5	0.15	$0.70^{\pm 0.04}$	$1.23^{\pm 0.10}$	$2205^{\pm 100}$	10.1	1432	1677	−23	4
Czernik	6	02	02	00	62	50	00	2.6	0.66	$0.25^{\pm 0.06}$	$1.00^{\pm 0.10}$	$2530^{\pm 115}$	10.3	1656	1912	47	4
Czernik	7	02	02	24	62	15	00	2.5	0.31	$0.10^{\pm 0.01}$	$1.19^{\pm 0.11}$	$2235^{\pm 100}$	10.1	1469	1684	20	4
Czernik	10	02	33	54	60	10	00	2.2	0.06	$0.20^{\pm 0.02}$	$1.71^{\pm 0.13}$	$1575^{\pm 70}$	9.7	1120	1107	−6	4
Czernik	11	02	36	35	59	38	00	3.0	0.26	$0.35^{\pm 0.03}$	$1.00^{\pm 0.10}$	$1210^{\pm 55}$	9.4	868	842	−12	4
Czernik	12	02	39	12	54	55	00	3.0	0.85	$0.40^{\pm 0.02}$	$0.45^{\pm 0.07}$	$2090^{\pm 95}$	10.2	1550	1392	−173	4
Czernik	14	03	16	54	58	36	00	2.0	0.03	$0.25^{\pm 0.07}$	$1.71^{\pm 0.13}$	$2175^{\pm 100}$	10.3	1688	1371	35	4
Czernik	15	03	23	12	52	15	00	2.4	0.21	$0.02^{\pm 0.00}$	$1.00^{\pm 0.10}$	$1155^{\pm 55}$	9.5	945	659	−80	4
Czernik	16	03	30	48	52	39	00	5.0	0.55	$0.20^{\pm 0.03}$	$1.29^{\pm 0.10}$	$2580^{\pm 120}$	10.7	2132	1447	−134	4
Czernik	17	03	52	24	61	57	00	3.6	0.39	$0.40^{\pm 0.04}$	$0.87^{\pm 0.05}$	$2120^{\pm 95}$	10.3	1673	1281	228	4
Czernik	25	06	13	06	06	59	00	5.0	0.60	$0.13^{\pm 0.02}$	$0.58^{\pm 0.07}$	$1980^{\pm 90}$	10.4	1824	−748	−181	4
Czernik	26	06	30	48	−04	13	00	2.7	0.08	$0.17^{\pm 0.02}$	$0.45^{\pm 0.06}$	$1200^{\pm 55}$	9.5	984	−673	−136	4
Czernik	30	07	31	18	−09	58	00	3.6	0.32	$0.13^{\pm 0.01}$	$0.35^{\pm 0.04}$	$2275^{\pm 105}$	10.2	1566	−1642	165	4
Czernik	37	17	53	17	−27	22 1	0	1.8	0.10	$0.60^{\pm 0.03}$	$1.03^{\pm 0.10}$	$1730^{\pm 80}$	6.77	−1728	67	−19	1
Czernik	38	18	49	42	04	56	00	5.0	0.11	$0.01^{\pm 0.00}$	$2.03^{\pm 0.36}$	$1910^{\pm 90}$	7.1	−1521	1152	88	4
Czernik	39	19	07	44	04	20	00	2.5	0.04	$0.01^{\pm 0.00}$	$2.90^{\pm 0.45}$	$1340^{\pm 60}$	7.5	−1046	836	−38	4
Czernik	42	22	39	48	59	54	54	3.5	0.46	$0.01^{\pm 0.00}$	$1.74^{\pm 0.12}$	$2585^{\pm 120}$	9.6	761	2470	52	4
Czernik	44	23	33	30	61	57	00	4.0	0.08	$0.16^{\pm 0.04}$	$1.48^{\pm 0.10}$	$3450^{\pm 160}$	10.4	1398	3154	27	4
Czernik	45	23	56	18	64	33	00	2.5	0.19	$0.02^{\pm 0.00}$	$1.45^{\pm 0.11}$	$2530^{\pm 115}$	9.9	1150	2251	102	4
Dol-Dzim	1	02	47	30	17	16	00	7.0	0.16	$5.00^{\pm 0.25}$	$0.10^{\pm 0.03}$	$960^{\pm 45}$	9.4	710	278	−584	4
Dol-Dzim	2	05	23	4	11	28	00	5.0	0.38	$0.80^{\pm 0.03}$	$0.65^{\pm 0.11}$	$1220^{\pm 55}$	9.7	1159	−251	−286	4
Dol-Dzim	3	05	33	42	26	29	00	4.5	0.19	$0.40^{\pm 0.02}$	$0.77^{\pm 0.13}$	$2530^{\pm 115}$	11.0	2525	−30	−v156	4
Dol-Dzim	4	05	35	54	25	57	00	12.0	0.26	$0.10^{\pm 0.00}$	$1.10^{\pm 0.18}$	$1220^{\pm 55}$	9.7	1217	−30	−73	4
Dol-Dzim	5	16	27	24	38	04	00	15.0	0.55	$2.0^{\pm 0.09}$	$0.02^{\pm 0.00}$	$900^{\pm 40}$	8.1	−316	567	624	4
Dol-Dzim	6	16	45	24	38	21	00	4.0	0.53	$5.0^{\pm 0.26}$	$0.03^{\pm 0.00}$	$820^{\pm 35}$	8.1	−297	549	531	4
Dol-Dzim	7	17	10	36	15	32	00	3.0	0.88	$2.0^{\pm 0.11}$	$0.13^{\pm 0.02}$	$1140^{\pm 50}$	7.6	−802	589	555	4
Dol-Dzim	8	17	26	12	24	11	00	8.0	0.90	$3.0^{\pm 0.12}$	$0.06^{\pm 0.00}$	$2330^{\pm 100}$	7.1	−1392	1494	1123	4
Dol-Dzim	9	18	08	48	31	32	00	12.0	0.30	$2.3^{\pm 0.10}$	$0.06^{\pm 0.00}$	$2330^{\pm 100}$	7.6	−1091	1752	845	4
Dol-Dzim	10	20	05	48	40	32	00	2.5	0.07	$1.0^{\pm 0.05}$	$0.55^{\pm 0.09}$	$1670^{\pm 75}$	8.3	−384	1620	135	4
Dol-Dzim	11	20	51	00	35	57	00	3.0	0.40	$2.0^{\pm 0.11}$	$0.42^{\pm 0.05}$	$2545^{\pm 115}$	8.4	−522	2480	−232	4
Ruprecht	13	07	08	03	−25	52	00	4.5	0.07	$1.00^{\pm 0.05}$	$0.26^{\pm 0.05}$	$1300^{\pm 60}$	9.3	685	−1090	−185	9
Ruprecht	15	07	19	33	−19	38	00	5.5	0.32	$0.50^{\pm 0.03}$	$0.65^{\pm 0.05}$	$1845^{\pm 85}$	9.7	1095	−1482	−93	8
Ruprecht	16	07	23	10	−19	28	00	3.5	0.31	$0.16^{\pm 0.02}$	$0.71^{\pm 0.07}$	$2160^{\pm 100}$	9.9	1276	−1742	−78	9
Ruprecht	24	07	31	54	−12	45	00	5.0	0.54	$0.06^{\pm 0.00}$	$0.35^{\pm 0.05}$	$1983^{\pm 90}$	9.9	1300	−1492	103	9
Ruprecht	135	17	58	12	−11	39	00	3.0	0.50	$0.50^{\pm 0.02}$	$1.10^{\pm 0.05}$	$1850^{\pm 85}$	6.74	−1764	520	201	1
Ruprecht	137	18	00	16	−25	13	39	2.8	0.25	$0.80^{\pm 0.06}$	$0.67^{\pm 0.05}$	$1450^{\pm 65}$	7.06	−1445	123	−23	1
Ruprecht	138	17	59	56	−24	40	57	3.0	0.21	$2.00^{\pm 0.11}$	$0.18^{\pm 0.05}$	$930^{\pm 40}$	7.57	−926	86	−9	1
Ruprecht	142	18	32	11	−12	13	47	3.3	0.03	$0.40^{\pm 0.04}$	$0.91^{\pm 0.05}$	$1735^{\pm 80}$	6.89	−1631	590	−41	1
Ruprecht	168	17	52	46	−28	26	00	2.6	0.80	$2.00^{\pm 0.12}$	$1.06^{\pm 0.11}$	$820^{\pm 35}$	7.68	−820	18	−16	1
Ruprecht	169	17	59	22	−24	46	01	2.6	0.14	$1.00^{\pm 0.05}$	$0.66^{\pm 0.05}$	$1390^{\pm 60}$	7.12	−1384	125	−13	1
Ruprecht	171	18	32	11	−16	02	59	5.7	0.26	$3.20^{\pm 0.15}$	$0.12^{\pm 0.03}$	$1140^{\pm 50}$	7.41	−1092	323	−62	1
Dolidze	9	20	25	42	41	56	00	3.0	0.72	$0.02^{\pm 0.00}$	$0.80^{\pm 0.05}$	$866^{\pm 40}$	8.4	−152	852	35	5
Dolidze	10	20	26	18	40	07	00	1.8	0.32	$0.25^{\pm 0.05}$	$0.80^{\pm 0.05}$	$950^{\pm 44}$	8.4	−190	931	19	5
Dolidze	11	20	26	30	41	27	00	2.5	0.27	$0.40^{\pm 0.03}$	$0.83^{\pm 0.06}$	$1127^{\pm 52}$	8.4	−204	1108	37	5
Dolidze	19	05	23	42	08	11	00	12.0	0.40	$0.16^{\pm 0.05}$	$0.55^{\pm 0.02}$	$1320^{\pm 60}$	9.8	1229	−332	−349	5

(*continued on next page*)

Table 1 (*continued*)

Cluster		α			δ			$R_{lim.}$	R_c	Age	E_{B-V}	$R_\odot$	R_{gc}	$X_\odot$	$Y_\odot$	Z	Ref.
		h	*m*	*s*	°	′	″	′	′	*Gyr*	*mag*	*pc*	*kpc*	*pc*	*pc*	*pc*	
Dolidze	21	05	27	24	07	04	00	6.0	0.65	$0.20^{\pm 0.08}$	$0.55^{\pm 0.03}$	$1447^{\pm 65}$	9.9	1339	−399	−377	5
Dolidze	26	07	30	06	11	54	00	11.0	0.80	$0.10^{\pm 0.01}$	$0.44^{\pm 0.04}$	$1907^{\pm 88}$	10.2	1657	−826	458	5
Dolidze	27	16	36	30	−08	57	00	14.0	0.78	$0.05^{\pm 0.00}$	$0.75^{\pm 0.07}$	$1015^{\pm 45}$	7.5	−914	122	424	5
Dolidze	37	20	03	00	37	41	00	4.0	0.40	$0.30^{\pm 0.08}$	$0.48^{\pm 0.05}$	$1490^{\pm 70}$	8.2	−411	1429	93	5
Dolidze	39	20	16	24	37	52	00	4.0	0.06	$0.25^{\pm 0.06}$	$0.44^{\pm 0.05}$	$872^{\pm 40}$	8.3	−218	844	22	5
Dolidze	41	20	18	49	37	45	00	5.0	0.25	$0.40^{\pm 0.05}$	$0.53^{\pm 0.03}$	$1763^{\pm 80}$	8.2	−435	1708	31	5
Dias	2	06	09	09	04	35	24	5.5	0.41	$0.79^{\pm 0.02}$	$0.61^{\pm 0.11}$	$2835^{\pm 130}$	11.2	2570	−1142	−358	3
Dias	3	07	10	28	−08	26	14	8.0	0.88	$1.41^{\pm 0.11}$	$0.64^{\pm 0.11}$	$4650^{\pm 215}$	12.3	3423	−3147	28	3
Dias	4	13	43	40	−63	01	30	3.2	0.04	$1.26^{\pm 0.09}$	$0.60^{\pm 0.10}$	$2150^{\pm 100}$	7.3	−1347	−1675	−28	3
Dias	6	18	30	30	−12	18	59	3.0	0.28	$0.60^{\pm 0.02}$	$0.91^{\pm 0.07}$	$1580^{\pm 70}$	7.03	−1488	530	−28	1
Dias	7	19	49	22	21	09	48	5.0	0.22	$2.00^{\pm 0.10}$	$0.42^{\pm 0.04}$	$2540^{\pm 115}$	7.5	−1334	2158	−109	3
Dias	8	19	52	07	11	37	54	5.0	0.12	$2.24^{\pm 0.10}$	$0.30^{\pm 0.05}$	$2220^{\pm 100}$	7.3	−1404	1693	−302	3
Turner	2	18	17	11	−18	49	27	3.8	0.87	$0.10^{\pm 0.01}$	$0.36^{\pm 0.04}$	$1190^{\pm 55}$	7.34	−1163	250	−27	1
Turner	6	10	59	01	−59	29	58	1.3	0.11	$0.08^{\pm 0.01}$	$1.32^{\pm 0.13}$	$3250^{\pm 145}$	8.0	278	−3071	18	4
Turner	7	14	32	33	−56	53	12	13.0	0.32	$0.08^{\pm 0.01}$	$1.39^{\pm 0.15}$	$1800^{\pm 80}$	7.3	−251	−1238	104	4
Turner	8	19	45	16	27	50	30	5.0	0.34	$5.00^{\pm 0.30}$	$1.16^{\pm 0.12}$	$2160^{\pm 100}$	7.8	−30	1933	64	4
Turner	11	20	43	24	35	35	18	8.2	0.45	$0.40^{\pm 0.03}$	$1.13^{\pm 0.10}$	$1905^{\pm 85}$	8.3	−30	1850	−142	4
King	17	05	08	24	39	05	00	2.8	0.16	$0.79^{\pm 0.03}$	$0.73^{\pm 0.12}$	$2960^{\pm 135}$	11.4	2887	650	−38	3
King	18	22	52	06	58	17	00	2.4	0.16	$0.35^{\pm 0.03}$	$0.52^{\pm 0.07}$	$1860^{\pm 85}$	9.2	567	1770	−33	3
King	23	07	21	47	−00	59	06	3.6	0.37	$0.89^{\pm 0.04}$	$0.16^{\pm 0.05}$	$3113^{\pm 140}$	11.2	2513	−1795	390	3
King	26	19	29	01	14	52	02	2.2	0.24	$0.44^{\pm 0.02}$	$1.27^{\pm 0.15}$	$2600^{\pm 120}$	7.1	−1656	2003	−61	3
BH	47	08	42	33	−48	05	13	7.7	0.27	$0.80^{\pm 0.05}$	$0.73^{\pm 0.05}$	$2465^{\pm 110}$	6.03	145	−2456	−154	1
BH	60	09	15	53	−50	00	38	2.1	0.09	$0.40^{\pm 0.01}$	$0.67^{\pm 0.05}$	$1325^{\pm 60}$	7.17	−38	−1324	−16	1
BH	218	17	16	12	−39	24	04	2.8	0.06	$0.40^{\pm 0.01}$	$0.88^{\pm 0.06}$	$1215^{\pm 55}$	7.28	−1188	−254	−14	1
ESO	524−01	18	56	37	−26	57	39	3.0	0.30	$3.20^{\pm 0.14}$	$0.30^{\pm 0.03}$	$2800^{\pm 130}$	5.75	−2694	430	−629	1
ESO	522−05	18	12	53	−24	21	50	2.2	0.23	$3.20^{\pm 0.14}$	$1.82^{\pm 0.15}$	$660^{\pm 30}$	7.84	−654	80	−35	1
ESO	525−08	19	27	16	−23	34	35	3.0	0.26	$1.00^{\pm 0.05}$	$0.36^{\pm 0.04}$	$1640^{\pm 75}$	6.93	−1505	407	−507	1
IC	1434	22	10	34	52	49	40	3.5	0.27	$0.32^{\pm 0.02}$	$0.66^{\pm 0.05}$	$3035^{\pm 140}$	9.5	523	2986	−143	3
IC	2156	06	04	51	24	09	30	2.0	0.07	$0.25^{\pm 0.02}$	$0.67^{\pm 0.05}$	$2100^{\pm 95}$	10.6	2087	−230	47	3
IC	4291	13	36	56	−62	05	45	2.8	0.09	$0.80^{\pm 0.04}$	$0.61^{\pm 0.05}$	$1790^{\pm 82}$	7.53	−1107	−1406	10	1
Alessi	15	06	43	04	01	40	19	6.0	0.12	$0.45^{\pm 0.03}$	$0.91^{\pm 0.07}$	$2509^{\pm 116}$	10.74	2161	−1273	−48	7
Alessi	53	06	29	24	09	10	39	6.4	0.13	$0.50^{\pm 0.04}$	$0.61^{\pm 0.05}$	$2360^{\pm 109}$	10.72	2184	−894	−27	7
Juchert	1	19	22	32	12	40	00	1.6	0.04	$0.40^{\pm 0.03}$	$1.36^{\pm 0.10}$	$2286^{\pm 105}$	7.16	−1538	1691	−40	7
Juchert	12	07	20	57	−22	52	00	5.0	0.36	$0.30^{\pm 0.02}$	$0.91^{\pm 0.07}$	$3016^{\pm 139}$	10.47	1658	−2510	−217	7
Riddle	4	02	07	23	60	15	25	2.2	0.13	$0.05^{\pm 0.05}$	$0.91^{\pm 0.07}$	$1993^{\pm 92}$	9.95	1339	1475	−43	7
Riddle	15	19	11	09	14	50	04	2.5	0.08	$0.50^{\pm 0.03}$	$1.33^{\pm 0.10}$	$1925^{\pm 89}$	7.36	−1278	1437	82	7
Skiff	1	06	14	47	12	52	15	1.5	0.10	$0.25^{\pm 0.01}$	$0.57^{\pm 0.04}$	$3150^{\pm 145}$	5.35	3005	−937	−115	1
Skiff	2	04	58	14	43	00	48	2.5	0.30	$0.90^{\pm 0.06}$	$0.18^{\pm 0.05}$	$2125^{\pm 100}$	6.37	2032	621	5	1
Teutsch	11	06	25	24	13	51	59	3.0	0.26	$0.50^{\pm 0.04}$	$0.70^{\pm 0.05}$	$3443^{\pm 159}$	11.83	3280	−1044	39	7
Teutsch	144	21	21	44	50	36	36	5.0	0.30	$0.80^{\pm 0.08}$	$0.73^{\pm 0.05}$	$1704^{\pm 79}$	8.75	81	1702	14	7
Collinder	351	17	49	00	−28	44	09	4.2	0.19	$0.16^{\pm 0.02}$	$0.70^{\pm 0.05}$	$1310^{\pm 60}$	7.19	−1310	14	−16	1
Patchick	89	19	59	33	49	18	45	3.5	0.07	$1.60^{\pm 0.13}$	$0.21^{\pm 0.02}$	$2646^{\pm 122}$	8.62	−288	2588	465	7
Toepler	1	20	01	18	33	36	54	4.0	0.10	$0.40^{\pm 0.03}$	$0.79^{\pm 0.05}$	$2890^{\pm 133}$	8.00	−974	2719	87	7

Table 2 References of studied clusters.

Number	Reference
1	Tadross (2008a)
2	Tadross (2008b)
3	Tadross (2009a)
4	Tadross (2009b)
5	Tadross and Nasser (2010)
6	Tadross (2011)
7	Tadross et al. (2012)
8	Tadross (2012a)
9	Tadross (2012b)

open clusters in the Galaxy based on the *2MASS* database. Froebrich (2010) studied 269 open clusters; ages, core radii, reddening, Galactocentric distances and the scale-heights were determined. Similar to this kind of study, Schilbach (2006) derived the linear sizes of some 600 clusters and investigated the effect of the mass segregation of stars in open clusters. Bica et al. (2003) researched 346 open clusters, based on the *2MASS* database; they studied the linear diameters and spatial distribution of open clusters in the Galaxy. Tadross (2001, 2002) studied 160 open clusters used *UBV-CCD* observations and derived the relationships projected onto the Galactic plane in morphological way. Dutra and Bica (2001) studied 42 new infrared star clusters, stellar groups and candidates towards the Cyngus X region. Dutra and Bica (2000) have studied 103 Galactic open clusters and compared the reddening values obtained from far infrared *IRAS* and *COBE* observations with those obtained from visible observations. Dambis (1999) determined the main parameters of 203 open clusters based on the published photoelectric and CCD data. Malysheva (1997) published a Catalogue of parameters for 73 open clusters determined from uvbyβ photometry; his values are in good agreement with those of Loktin and Matkin (1994). Loktin (1997) published their improved version Catalogue, which contained the updated parameters of homogeneously estimated excesses, distances, and ages for 367 open clusters. Friel (1995) and Janes and Phelps (1994) based on a sample of some 70 objects investigated how the extinction and age depend on the position in the Galaxy. Also, a comparison between the age and position in the Galaxy was studied by Lyngå (1980), Lyngå (1982). In addition an old study of Janes (1979) used UBV photometry to study the reddening and metallicity of 41 open clusters.

3. Data analysis

The current study depended mainly on the correlations between the astrophysical parameters of 263 open star clusters of different names listed as follows: 124 clusters of NGC; 24 objects of Berkeley; 23 of Kronberger; 23 of Czernik; 11 of Dol-Dzim; 11 of Ruprecht; 10 of Dolidze; 6 of Dias; 5 of Turner; 4 of King; 3 of BH; 3 of Eso; 3 of IC; 2 of Alessi; 2 of Juchert; 2 of Riddle; 2 of Skiff; 2 of Teutsch; 1 of Collinder; 1 of Patchick; and 1 cluster of Toepler.

This sample contains clusters with ages in the range from 5 Myr to 5 Gyr. They are located at distances up to 4.7 kpc from the Sun ($R_{\odot}$), up to 12.5 kpc from the Galactic Centre (R_{gc}), and less than ± 2 kpc from the Galactic Plane (Z). They range from 0.25 to 16.5 arcmin in limiting radii ($R_{lim.}$), and up to 1 arcmin in core radii (R_c); with noticing that the estimated $R_{lim.}$ and R_c in parsecs depending mainly on the distance of the clusters individually.

Data extraction has been performed for each cluster using the known tool of VizieR for *2MASS*.[1] Point Source Catalogue database of Skrutskie (2006). The investigated clusters have been selected from WEBDA and DIAS databases under some conditions mentioned in our last series papers. It is noticed that most clusters' sizes seem to be greater in the infrared band (*2MASS* observations) than in the optical band; because this system can detect the very faint stars, even those behind the curtains of interstellar matter. The real spatial distribution of open clusters along the Milky Way Galaxy refers to some paucity of the clusters at G. longitudes range from 140° to 200°. The lack of objects in that direction is noticed also in earlier studies and confirmed for open clusters by Benjamin (2008), and Bukowiecki (2011). Older clusters seem to be more dispersed than younger ones of the Hyades, as shown in the left panel of Fig. 1. The relationships between the astrophysical parameters of open clusters are presented here with respect to their ages and places, so then the astrophysical behaviour of open clusters along the Milky Way Galaxy can be investigated.

4. Limiting and core radii

One of the main tasks in this work was the determination of the radial density profile (RDP) for each cluster, i.e. the observed stellar density ρ that was plotted as a function of the angular radial distance from the cluster centre, King (1966):

$$\rho(r) = f_{bg} + \frac{f_0}{1 + (R_{lim}/R_c)^2}$$

where R_c,f_0, and f_{bg} are the core radius, the central density, and the background density, respectively. The core radius was derived as a distance where the stellar density drops to half of f_0. The parameters were derived with the least-square method. The cluster's limiting radius, R_{lim}, was defined by comparing $\rho(r)$ with the background density level ρ_{bg}, (cf. Bukowiecki, 2011). From both R_c and R_{lim}, one can estimate the concentration parameter $c = log(R_{lim}/R_c)$, Peterson and King (1975). This parameter can be added as a new item to characterize the structure of clusters along the Galaxy. In the present work, the concentration parameters are ranging from 0.39 to 2.5. In this context, Nilakshi (2002) concluded that the angular size of the coronal region is about 6 times the core radius, while Maciejewski and Niedzielski (2007) reported that R_{lim} may vary for individual clusters from $2R_c$ to $7R_c$. In our case, for the whole sample, the average values of limiting radius, core radius, and concentration parameter are 4.6 arcmin, 0.3 arcmin, and 1.2, respectively. We concluded that $R_{lim} = 6.85R_c$; for the clusters up to $R_c = 0.5$ arcmin, and $R_{lim} = 2.88R_c$; for the clusters up to $R_c = 1.0$ arcmin. i.e, our conclusion is almost in agreement with Maciejewski and Niedzielski (2007).

5. Main photometric parameters

Depending on the *2MASS* data, deep stellar analyses of the candidate clusters have been presented. The photometric data

[1] http://vizier.u-strasbg.fr/viz-bin/VizieR?-source=2MASS.

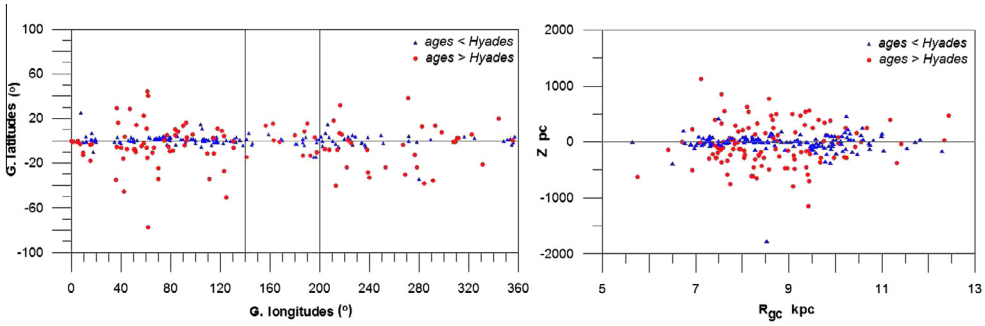

Fig. 1 Left panel represents the clusters' distribution according to their Galactic longitudes and latitudes, the dark area refers to the paucity of the clusters at G. longitudes ranging from 140^o to 200^o. Right panel represents the clusters' distribution according their distances from the Galactic centre, R_{gc}, and Galactic plane, Z, assuming that $Z_\odot = -33$ pc, and $R_{gc_\odot} = 8.5$ kpc for the Sun. Both panels plotted for two ranges of clusters' ages, younger and older than Hyades.

of *2MASS* not only allow us to construct relatively well defined CM diagrams of the clusters, but also permit a more reliable determination of astrophysical parameters. In this paper, we used extraction areas having a radius of 20 arcmin, which are larger than the estimated limiting radius of the clusters. Because of the weak contrast between the cluster and the background field density, some inaccurate statistical results may be produced beyond the real limit of cluster borders (Tadross, 2005).

The main astrophysical parameters of the clusters, e.g. age, reddening, distance modulus, can be determined by fitting the isochrones to the cluster CMDs. To do this, we applied several fittings on the CMDs of the clusters by using the stellar evolution models of Marigo (2008) of Padova isochrones on the solar metallicity. It is worth mentioning that the assumptions of solar metallicity are quite adequate for young and intermediate age open clusters, which are closer to the Galactic disc. So, Near-Infrared surveys are very useful for the investigation of such clusters. It is relatively less affected by high reddening from the Galactic plane. However, for specific age isochrones, the fit should be obtained at the same distance modulus for both diagrams [J–(J–H) & K_s–(J–K_s)], and the colour excesses should obey Fiorucci and Munari's (2003) relations for normal interstellar medium. We note that, it is difficult to obtain some accurate determinations of the astrophysical parameters due to the weak contrast between clusters and field stars.

Reddening determination is one of the major steps in the cluster compilation. Therefore, we used Schlegel (1998) as a guide for estimating reddening. In this context, for colour excess transformations, we used the coefficient ratios $\frac{A_J}{A_V} = 0.276$ and $\frac{A_H}{A_V} = 0.176$, which were derived from absorption ratios in Schlegel (1998), while the ratio $\frac{A_{K_s}}{A_V} = 0.118$ was derived from Dutra (2002). Applying the calculations of Fiorucci and Munari (2003) for the colour excess of *2MASS* photometric system; we ended up with the following results: $\frac{E_{J-H}}{E_{B-V}} = 0.309 \pm 0.130$, $\frac{E_{J-K_s}}{E_{B-V}} = 0.485 \pm 0.150$, where $R_V = \frac{A_V}{E_{B-V}} = 3.1$. Also, we can de-redden the distance modulus using these formulae: $\frac{A_J}{E_{B-V}} = 0.887$, $\frac{A_{K_S}}{E_{B-V}} = 0.322$. Then the distance of each cluster from the Sun, $R_\odot$, can be calculated. Consequently, the distance from the Galactic plane ($Z_\odot$), and the projected distances in the Galactic plane from the Sun ($X_\odot$&$Y_\odot$) can be determined, see Table 3. For more details about the distance calculations, see Tadross (2011).

6. Ages and locations

The distribution of our sample according to the distances from the Galactic centre, Rgc, and the height from the Galactic plane, Z, is presented in the right panel of Fig. 1. We can see that the clusters with ages younger than Hyades, i.e. less than $(7 \times 10^8$ yr) are strongly concentrated to the Galactic plane. While the clusters which are older than Hyades are more dispersed from the Galactic plane (cf. Friel, 1995). However, the correlations of the clusters' ages and locations with the other properties along the Milky Way Galaxy are presented in the following sections.

7. Reddening distribution

In fact reddening affects the distance determination via the main sequence fitting, actually it affected all the clusters' dimensions and positions on the Galaxy (cf. Tadross, 2002). The distribution of the reddening of our sample versus the Galactic latitudes confirms that the higher values of reddening are concentrated on and near the Galactic plane as shown in Fig. 2. Along the Galactic longitude bins of 20° the distribution of the mean reddening at each bin shows that the higher values are concentrated around the longitude range from 345° to 130°, i.e. in the directions of the Galactic centre and Sagittarius arm, as shown in Fig. 3. The general trend of reddening with age shows that reddening decreases with ages

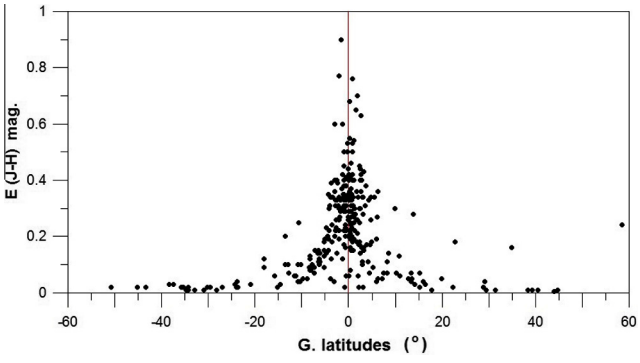

Fig. 2 The distribution of the reddening versus the Galactic latitudes.

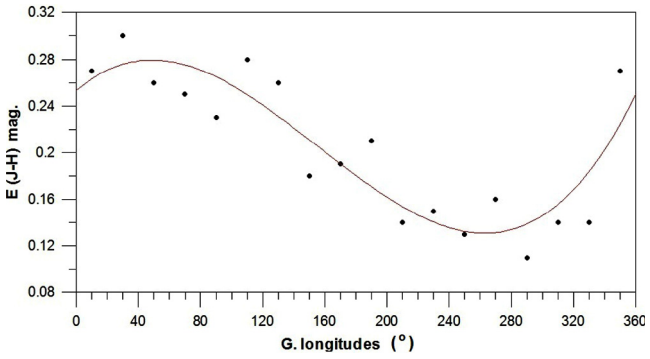

Fig. 3 The distribution of the mean reddening along the Galactic longitude bins of 20° for each.

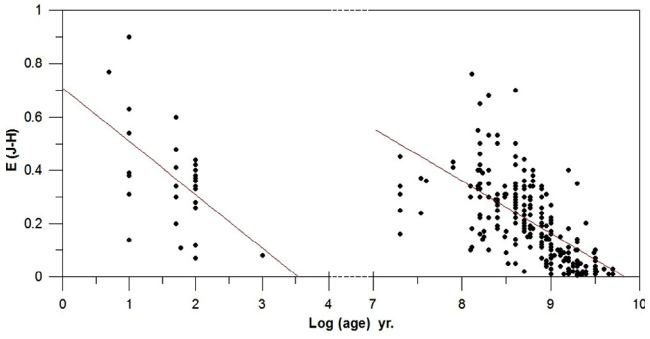

Fig. 4 The relation between the clusters' ages and reddening. Left and right panels represent the very young and old clusters respectively.

where younger clusters tend to be more reddened than older ones, see Fig. 4. On the other hand, the relation between reddening and R_{gc} reveals that the clusters inside the galactocentric radius of the Sun ($R_{gc_\odot} = 8.5$ kpc) have higher values of reddening than that of outside ones, as shown in Fig. 5. This confirms to some extent that the Sun's vicinity clusters are young and medium ones than those outside clusters.

8. Diameters' relations

The linear diameters have been plotted versus the absolute values of the height from the Galactic plane |Z|, and the distance from the Galactic centre R_{gc} as shown in Figs. 6 and 7, respectively. We can see that most clusters with typical diameters ($D < 10$ pc) are concentrated near the Galactic plane, especially those inside the galactocentric radius of the Sun $R_{gc} \leqslant 8.5$ kpc. The general trend of this relation appears that large, old clusters are found far from R_{gc} – it is confirmed by Bukowiecki (2011) – and also at large height Z (Tadross, 2002). Some young clusters with larger diameters are belonging to the Galactic plane are founded loose and unbound objects. The relation between the diameters and the galactocentric radii has been examined to be:

$$\text{Diam.} = 0.53R_{gc} - 0.19$$

The standard error of this relation ≈3.0

Burki and Maeder (1976) found a correlation between these quantities only for the very young clusters, but we have found such correlation for intermediate and older clusters as well.

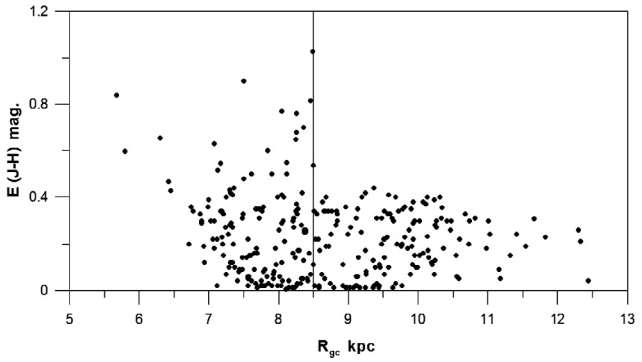

Fig. 5 The relation between the reddening and distance from the Galactic centre R_{gc}. The vertical line represents the galactocentric radius of the Sun, assuming that $R_{gc_\odot} = 8.5$ kpc.

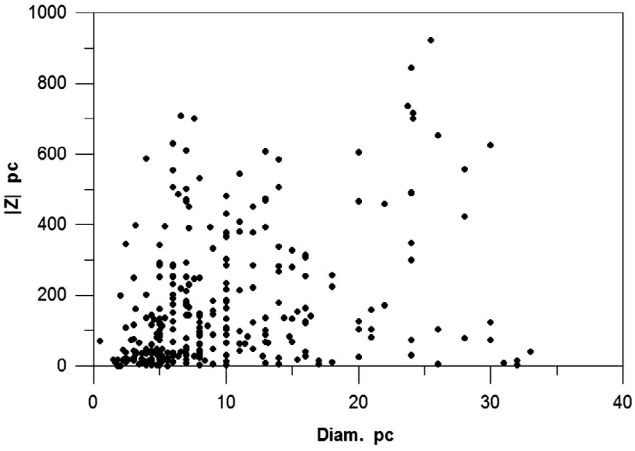

Fig. 6 The relation between the diameters and the absolute values of the height from the Galactic plane, |Z|.

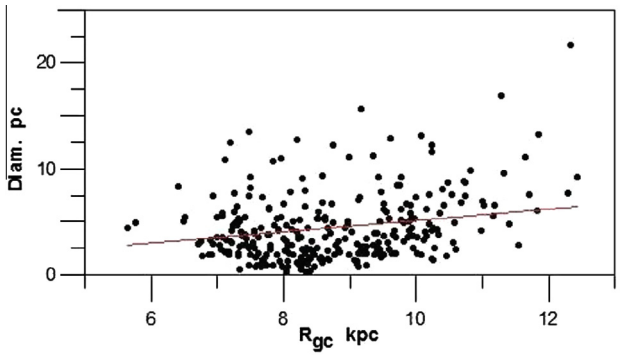

Fig. 7 The relation between the galactocentric radii, R_{gc}, and linear diameters of the clusters, assuming that $R_{gc_\odot} = 8.5$ kpc for the Sun. The standard error ≈ 3.0.

Fig. 8 represents the relation between ages and linear diameters of our sample. It can be expressed as follows:

$$\text{Diam.} = 3.18Log(age) - 18.53$$

The standard error of this relation ≈3.2

We can see that, to some extent, there is a correlation between diameters and ages, whereas clusters of large sizes

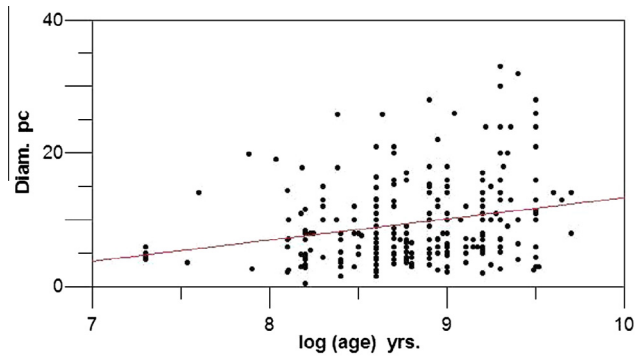

Fig. 8 The relation between ages and linear diameters of the studied clusters. The standard error ≈ 3.2.

belong to older ages, which have also large heights from Z. Youngest clusters with large sizes are supposed to be some groups of OB associations and probably they are not bound systems (Lyngå, 1982; Janes et al., 1988). Massive clusters with small sizes will be dissolved due to encounters among their members, while those of very large sizes with the same mass will be unstable in the Galactic tidal field, and they may take a very long time to have stability and relaxation (Theis, 2001). Small clusters with typical diameters less than 10 pc show a concentration to the Galactic plane (Wielen, 1971, 1975) in the range of $|Z| < 100$ pc, see Fig. 6, but larger clusters have both intermediate and old ages.

9. Ages' relations

The clusters' ages have been plotted versus Z, as shown in Fig. 9. Most clusters with ages $t \leq 10^{8.9}$ yr are lying around $|Z| \approx 200$ PC, while older ones are lying higher than such heights. It indicated that the thickness of the Galactic disc has not changed on the time scale of about $10^{9.0}$ yr and the clusters can be formed everywhere inside this layer (cf. Tadross, 2002). Lyngå and Palous (1987) have found that old clusters are much thicker distributed in the outer parts of the Galaxy than in the inner parts, Bukowiecki (2011). Also in our study the thickness of the Galactic disc increases for older clusters as well. Old clusters not only spend their time in the outer disc away from the disruptive effects of giant molecular clouds, but also, they spend their time at large distances from the Galactic plane, further enhancing their survivability (Friel, 1995).

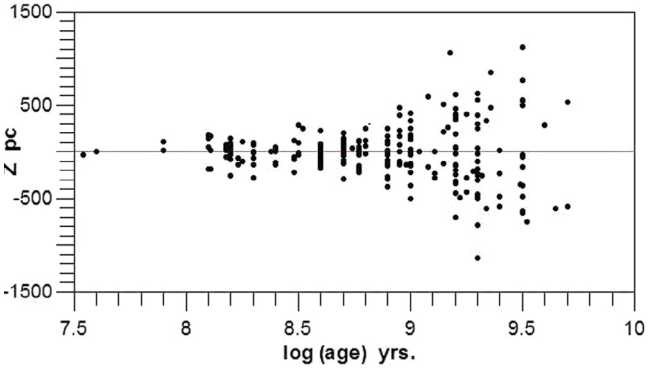

Fig. 9 The relation between ages and the heights from the Galactic plane, assuming that $Z_\odot = -33$ pc for the Sun.

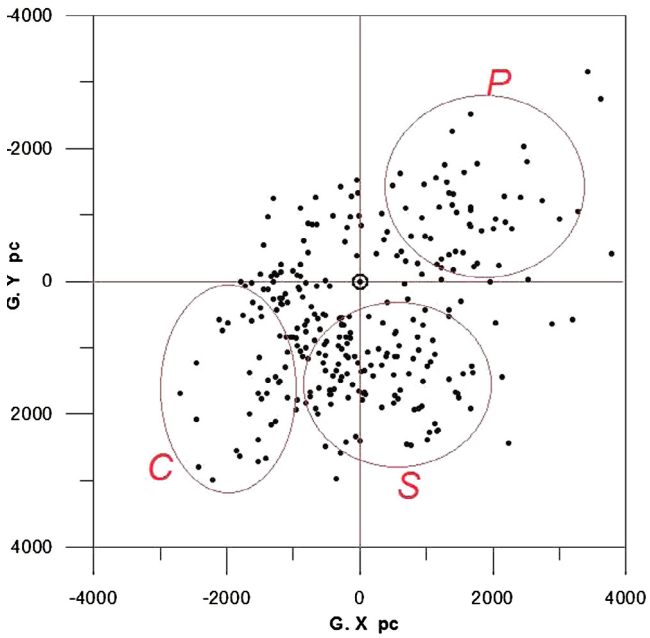

Fig. 10 The distribution of our sample on the Galactic plane. The three circles refer to the three famous arms of the Galaxy: Perseus (P), Sagittarius (S), and Carina (C).

On the other hand, the relation between ages and R_{gc} of the clusters implies that there is a lack of old clusters in the inner parts of the Galactic disc, and the anti-centre clusters survive longer than such clusters. In the inner parts of the Galaxy they have never gotten the relaxation state in the fluctuating gravitational field of that part (Lyngå, 1980; McClure, 1981; Vanden Bergh, 1985). The general trend reveals that, lifetime increases outwards the Milky Way Galaxy, where clusters live longer than those in the inner parts of it.

10. Galactic spiral arms

To show the shape of the spiral arms of the Galaxy, several studies have been carried out in the last five decades. The positions of the clusters on the Galactic plane have been used to trace the spiral arms of the Milky Way Galaxy. Centred on the Sun at ($X_\odot = Y_\odot = 0$) the distribution of the clusters on the Galactic plane has been plotted, as shown in Fig. 10. Within a radius of 4 kpc from the Sun (cf. Janes et al., 1988) the distribution of the studied clusters defines three concentration features which are related to the spiral structure of the Galaxy, i.e. Perseus, Sagittarius and Carina. It is assumed that there are more than three arms of the Galaxy but because of the patchy cloud and absorption effects we cannot detect them all!

11. Galactic warp

The effect of the Galactic warp may be declared from the distribution of the open clusters of our sample using the Galactic coordinates X and Y versus the height Z within ±2 kpc from the Galactic plane, as shown in Fig. 11. The directions of the

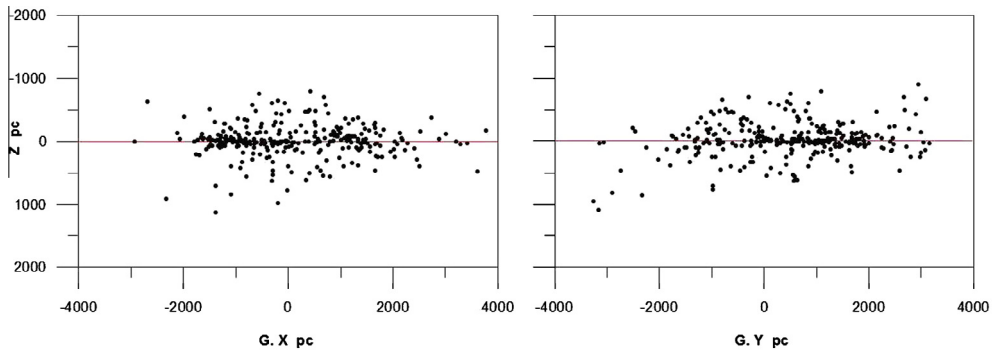

Fig. 11 The distribution of our sample according to their Galactic coordinates $X_\odot$ and $Y_\odot$ versus the height from the Galactic plane Z. The Sun's position is at $X_\odot = Y_\odot = 0$.

G. X and G. Y were defined to be positive in the direction of the Galactic radial centre and towards the direction of Galactic rotation respectively (Janes et al., 1988; Camerón, 1999; Piatti, 2003). No strong indication to the warp has been detected on the G. X direction, but, to some extent, it can be detected on the G. Y direction. This may refer to the leak of the studied clusters, especially those that have large distances from the Sun's vicinity (Tadross, 2002).

12. Conclusion

The results of our studied clusters in the last five years using near-infrared JHK_S photometric system are obtained here, and the correlations between the astrophysical parameters along the Milky Way Galaxy are achieved. It is obvious that (JHK_S) *2MASS* system affected the magnitude limit of the clusters, which detects many faint members located away from the cluster's core, so then the cluster seems to be larger than in optical bands. Detecting stars located in the lower parts of CMDs, makes the fitting with standard zero age main sequence much easier. This, of course, has contributed to the evaluation of the cluster parameters, i.e. distances, diameters, ages, reddening, etc. From our reduction, we concluded that $R_{lim} = 6.85R_c$; for the clusters up to $R_c = 0.5$ arcmin, and $R_{lim} = 2.88R_c$; for the clusters up to $R_c = 1.0$ arcmin, which are in agreement with Maciejewski and Niedzielski (2007). We also noticed that the linear size of open clusters increases with ages. The reddening decreases outward the Galactic plane, Z and the Galactic Center, R_{gc}, as well. This is noticed also for clusters located near the Sun vicinity and further than 8.5 kpc from the Galactic centre, i.e. the density of dust and gas decreases, too.

From our analysis, we noticed that the number of clusters decreases with Z; more than half of the studied clusters (52%) have aged less than 500 mega years and located at average age $|Z| = 75$ pc. Hence, the older ones are located at average $|Z| = 275$ pc, which is in agreement with Bukowiecki (2011). We can show that the difference between younger and older clusters can be declared in locations and sizes as the following relation:

$$\text{Diam.} = 0.53R_{gc} - 0.19 = 3.18Log(age) - 18.53$$

We found that the number of older clusters increases with R_{gc} and younger ones are obtained at an average $R_{gc} = 8.8$ kpc, which is confirmed by Tadross (2002), Froebrich (2010), and Bukowiecki (2011). The paucity of the clusters at G. longitudes ranging from 140^o to 200^o is noticeable by Tadross (2002), Benjamin (2008), Froebrich (2010), and Bukowiecki (2011). It may reflect the real spatial structure of the Milky Way Galaxy in that direction near the feature region of the Perseus arm (the external youngest arm of the Galaxy).

Acknowledgements

This publication makes use of data products from the Naval Observatory Merged Astrometric Dataset (*NOMAD*) and the Two Micron All Sky Survey *2MASS*, which is a joint project of the University of Massachusetts and the Infrared Processing and Analysis Centre/California Institute of Technology, funded by the National Aeronautics and Space Administration and the National Science Foundation. Catalogues from *CDS*/*SIMBAD* (Strasbourg), and Digitized Sky Survey *DSS* images from the Space Telescope Science Institute have been employed.

References

Benjamin, R.A., 2008. BAAS 40, 266.
Bica, E., Bonatto, Ch., Dutra, C.M., 2003. A&A 405, 991.
Bukowiecki, L. et al, 2011. Acta Astronom. 61, 231.
Burki, G., Maeder, A., 1976. A&A 51, 247.
Camerón, F., 1999. A&A 351, 506.
Dambis, A.K., 1999. Astron. Lett. 25, 7.
Dutra, C., Bica, E., 2000. A&A 359, 347.
Dutra, C., Bica, E., 2001. A&A 376, 434.
Dutra, C. et al, 2002. A&A 381, 219.
Fiorucci, M., Munari, U., 2003. A&A 401, 781.
Friel, E.D., 1995. Annu. Rev. Astron. Astrophys. 33, 381.
Froebrich, D. et al, 2010. MNRAS 409, 1281.
Janes, K.A., 1979. Astrophys. J. Suppl. 39, 135.
Janes, K., Tilley, C., Lyngå, G., 1988. Astron. J. 95, 771.
Janes, K.A., Phelps, R.L., 1994. AJ 108, 1773.
King, I., 1966. AJ 71, 64.
Loktin, A.V., Matkin, N., 1994. Astron. Astrophys. Trans. 4, 153.
Loktin, A.V. et al, 1997. Baltic Astron. 6, 316.
Lyngå, G., 1980. In: Hesser, J.E. (Ed.), IAU Symposium, 85, 13, Reidel, Dordrecht.
Lyngå, G., 1982. Astro. Astrophys. 109, 213.
Lyngå, G., Palous, J., 1987. Astro. Astrophys. 188, 35.
Maciejewski, G., Niedzielski, A., 2007. A&A 467, 1065.
Malysheva, L., 1997. Astron. Lett. 23, 585.
Marigo, P. et al, 2008. A&A 482, 883.
McClure, R. et al, 1981. Astrophys. J. 243, 841.

Nilakshi, S.R. et al, 2002. A&A 383, 153.
Peterson, C.J., King, I.R., 1975. AJ 80, 427.
Piatti, A. et al, 2003. MNRAS 346, 390.
Schilbach, E. et al, 2006. A&A 456, 523.
Schlegel, D. et al, 1998. ApJ 500, 525.
Skrutskie, M. et al, 2006. AJ 131, 1163.
Tadross, A.L., 2001. New Astron. 6 (5), 293.
Tadross, A.L. et al, 2002. New Astron. 7, 553.
Tadross, A.L., 2005. AN 326, 19.
Tadross, A.L., 2008a. New Astron. 13, 370.
Tadross, A.L., 2008b. MNRAS 389, 285.
Tadross, A.L., 2009a. New Astron. 14, 2000.
Tadross, A.L., 2009b. Astrophys. Space Sci. 323, 383.
Tadross, A.L., Nasser, M.A., 2010. NRIAG J. Ser. A67 (arXiv:1011.2934).
Tadross, A.L., 2011. JKAS 44 (1), 1.
Tadross, A.L. et al, 2012. RAA 12, 75.
Tadross, A.L., 2012a. RAA 12, 158.
Tadross, A.L., 2012b. New Astron. 17, 198.
Theis, Ch. 2001, Astronomische Gesellschaft Abs. Ser., 18, Annual Scientific Meeting JENAM 2001 # MS 05 47.
Vanden Bergh, D., 1985. Astrophys. Suppl. 58, 711.
Wielen, R., 1971. A&A 13, 309.
Wielen, R. 1975. In: Hayli, A. (Ed.), IAU Symposium, 69, 119, Reidel, Dordrecht.